

Numerical Renormalization Group Study of Quadrupole Kondo Effect with the Crystal-field Excited State

Yuki Kaneko* and Hirokazu Tsunetsugu†

The Institute for Solid State Physics, The University of Tokyo, Kashiwa, Chiba 277-8581, Japan

We have studied the quadrupolar Kondo effect for an impurity in cubic environment with taking account of a singlet excited state Γ_1 , which models a Pr^{3+} ion with a non-Kramers double ground state Γ_3 . We have used the numerical renormalization group approach and determined the phase diagram with varying quadrupole Kondo coupling J and Γ_1 excitation energy Δ . Two phases are found and identified as local Fermi liquid and non-Fermi liquid. This non-Fermi liquid phase is characteristic to the two-channel Kondo impurity, and a similar phase diagram has been also found in other extended quadrupole models. We have analyzed in detail the J -dependence of the Kondo temperature T_K near the phase boundary $J_c(\Delta)$ and found a nice scaling behavior with an stretched exponential form $T_K \sim \delta J^\alpha \exp(-\text{const.}/\sqrt{\delta J})$ where $\delta J \equiv J - J_c(\Delta)$. This differs from the standard scaling form and indicates that one needs to consider renormalization of multiple coupling constants.

The multi-channel Kondo effect was first discussed by Nozières and Blandin¹⁾ to take account of orbital degrees of freedom into the Kondo effect. The effect of multiple channels may lead to the non-Fermi liquid (NFL) ground state in contrast to the local Fermi liquid (LFL) state²⁾ in ordinary Kondo systems. Since then, many studies have been performed on the multi-channel Kondo effect, and its singular behavior has been theoretically elucidated using various approaches such as numerical renormalization group (NRG),³⁻⁵⁾ conformal field theory,⁶⁻⁹⁾ and Bethe ansatz.¹⁰⁻¹²⁾ However, it is not easy to find model materials modeling a two-channel Kondo effect, hindered by the instability of the NFL state against channel asymmetries.^{5,13,14)} Thus, the design of physical systems realizing such states is an important challenge in strongly correlated systems; as well as experimental verification of NFL state.

For realizing the two-channel Kondo effect, D. L. Cox proposed the use of a quadrupole moment of an ion with f^2 -electron configuration such as U^{4+} or Pr^{3+} , and this is called the quadrupolar Kondo effect. The Kondo coupling works in the orbital degrees of freedom, while conduction electron spins $\sigma \in \{\uparrow, \downarrow\}$ corresponds to the channel degrees of freedom. The double-fold degeneracy of their ionic ground state is a nonmagnetic one of non-Kramers type and guaranteed when their crystal field has a high symmetry.¹⁵⁻¹⁷⁾ Recent experiments reported a few behaviors suggesting the quadrupolar Kondo effect in the 1-2-20 compounds $\text{PrV}_2\text{Al}_{20}$ ¹⁸⁾ and $\text{PrIr}_2\text{Zn}_{20}$.^{19,20)} However, large intersite interactions modify their physical properties from the behaviors of the 2-channel impurity model. They are candidate materials realizing the quadrupolar Kondo lattice (QKL), and several of their properties are consistent with the theoretical predictions for the QKL's.²¹⁾ Furthermore, a recent experiment reported the impurity quadrupole Kondo effect in the diluted Pr system $\text{Y}_{1-x}\text{Pr}_x\text{Ir}_2\text{Zn}_{20}$.²²⁾

One should note one important point about the orbital symmetry of an impurity quadrupole in a lattice. We consider here the case of cubic lattice. Despite a discrete symmetry of the

crystal field, the quadrupole has the continuous $O(2)$ orbital symmetry, if the Γ_3 doublet alone is considered. Taking into consideration the singlet Γ_1 excited state, this elevated symmetry is reduced to Z_3 , which is equivalent to the lattice symmetry. As for quadrupole lattices, it was found that this Z_3 orbital anisotropy plays an important role of stabilizing various types of quadrupole orders.²³⁾ However, this effect has been neglected in most of the theoretical studies on the quadrupole Kondo effect, except for a few studies which have investigated their effects on the NFL state for a quadrupole model in either tetragonal or hexagonal crystal field. They used the NRG method²⁴⁻²⁶⁾ or a variational approach²⁷⁾ and found a non-vanishing part of the parameter space where the NFL state is stable. This contrasts to the instability of the NFL fixed point against an infinitesimal channel anisotropy.

In this paper, we study the quadrupole Kondo effect with a special attention on the effect of orbital Z_3 anisotropy. To this end, we consider an impurity with the excited Γ_1 singlet and ground-state Γ_3 doublet $\{|\Gamma_{3u}\rangle, |\Gamma_{3v}\rangle, |\Gamma_1\rangle\}$. Our model differs from those used in the previous studies. Koga and Shiba used a realistic model considering the total angular momentum $j_z = 5/2$ of conduction electrons.²⁴⁾ Their model is quite complicated and also has a lower symmetry since they considered hexagonal or tetragonal crystal field.

We will study an extended quadrupole Kondo model (EQKM) which includes the singlet excited state Γ_1 . Its NRG Hamiltonian reads

$$H_N = \Lambda^{1/2} H_{N-1} + \sum_{\alpha\sigma} (f_{N-1,\alpha\sigma}^\dagger f_{N\alpha\sigma} + \text{H.c.}), \quad (1a)$$

$$\Lambda^{1/2} H_0 = J \sum_{\sigma} [(f_{0u\sigma}^\dagger f_{0v\sigma} + f_{0v\alpha}^\dagger f_{0u\sigma}) Q_x + (n_{0u\sigma} - n_{0v\sigma}) Q_z] + \Delta |\Gamma_1\rangle \langle \Gamma_1|, \quad (1b)$$

where Δ is the excitation energy of the Γ_1 state. The chemical potential is set to 0 corresponding to the half-filled conduction band, and H_N has the particle-hole symmetry. $f_{n\alpha\sigma}^\dagger$ is the creation operator of the electron in an orbital $\alpha \in \{u, v\}$ with spin $\sigma \in \{\uparrow, \downarrow\}$ at the n -th site in Wilson chain³⁾ and $n_{0\alpha\sigma} = f_{0\alpha\sigma}^\dagger f_{0\alpha\sigma}$. $\Lambda = 3$ is the scaling factor at each RG step. The impurity quadrupole operators are defined as

*kaneko-yuki314@issp.u-tokyo.ac.jp

†tsune@issp.u-tokyo.ac.jp

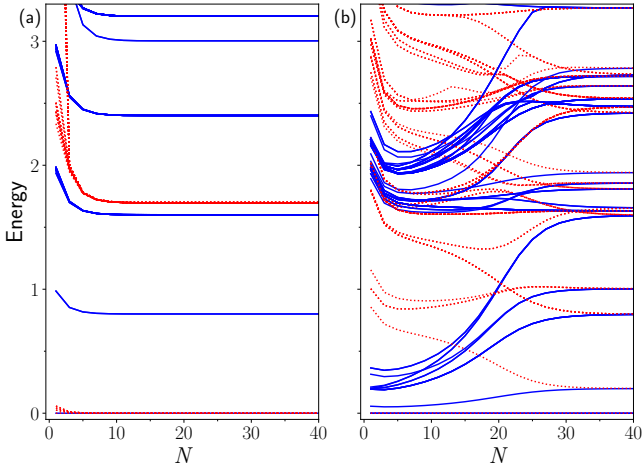


Fig. 1. (Color online) NRG energy flow of low-lying levels for $(J, \Delta) =$ (a) (1.0, 1.0) and (b) (0.1, 10). Data are shown by solid blue lines for even N and dotted red lines for odd N . $\Lambda = 3$.

$Q_z = |\Gamma_{3u}\rangle\langle\Gamma_{3u}| - |\Gamma_{3v}\rangle\langle\Gamma_{3v}| + (a|\Gamma_1\rangle\langle\Gamma_{3u}| + \text{H.c.})$ and $Q_x = (a|\Gamma_1\rangle - |\Gamma_{3u}\rangle)\langle\Gamma_{3v}| + \text{H.c.}$ with $a = \sqrt{35}/2$, and they constitute a basis set of the Γ_3 -irreducible representation (irrep) of the cubic point group.

We now discuss the symmetry of H_N . At each NRG step, we decompose the Hilbert space into subspaces using conserved quantities and diagonalize H_N in each subspace. Once H_0 includes the $Q_{z,x}$'s matrix elements involving Γ_1 , H_N loses the $O(2)$ symmetry in the Q_x - Q_z space, and thus its generator, $Q_y^{\text{tot}} = i(|\Gamma_{3u}\rangle\langle\Gamma_{3v}| + \sum_{n\sigma} f_{n\sigma}^\dagger f_{n\sigma}) + \text{H.c.}$, becomes non-conserved, while the $SU(2)$ spin rotation symmetry is unaffected. Thus, for subspace decomposition, we use the pair of quantum numbers $\{C\} = (C_\uparrow, C_\downarrow)$, where $C_\sigma = \sum_{0 \leq n \leq N} \sum_{\alpha=u,v} (f_{n\alpha\sigma}^\dagger f_{n\alpha\sigma} - 1/2)$ is the electron number for the spin direction σ minus $(N+1)$. In our NRG calculations, we retained about 1620 total states at each iteration N . We have also used a special trick to reduce numerical errors. Due to $SU(2)$ spin symmetry, the states with $S^{\text{tot}} > 0$ are necessarily degenerate among the subspaces $-S_z^{\text{tot}} \leq S_z^{\text{tot}} = \frac{1}{2}(C_\uparrow - C_\downarrow) \leq S_z^{\text{tot}}$. Thus, after diagonalization at each iteration, we reset the corresponding eigenenergies by their average value. This drastically improved the stability of NRG procedure. Without this trick, the system sometimes flows towards a false fixed point.

Identification of the phase requires the analysis of the RG fixed point. For each (J, Δ) -point, we start from H_0 and repeat NRG iterations until the low-energy spectrum converges. Figure 1(a) plots the RG energy flows for $(J, \Delta) = (1.0, 1.0)$ and this is the behavior of the LFL fixed point. The ground state is singlet with $\{C\} = (0, 0)$. The spectrum can be described by quasi-particle excitations, and thus the levels are equally separated by the single-particle energy $\eta_1 = 0.80041$. For even N , the first excited multiplet consists of the states with $\{C\} = (\pm 1, 0)$ or $(0, \pm 1)$, and each $\{C\}$ -state is doubly degenerate. The second (third) excited multiplet consists of the state with double- (triple-)particle excitations and has 28- (56-)fold degeneracy. For odd N , the multiplets specified by $\{C\}$ have now different energy. All of these results perfectly agree with the fixed-point spectrum of the spin-1 two-channel Kondo model,³⁾ and the ground state is identified as the LFL state.

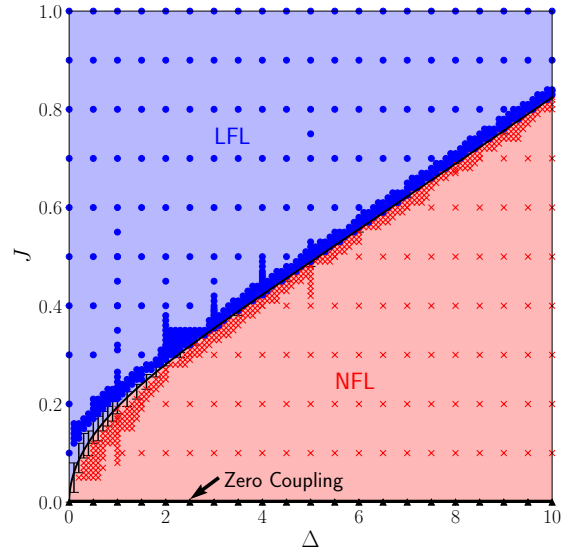


Fig. 2. (Color online) The phase diagram of EQKM. The LFL and NFL phases are marked by circles and crosses, respectively.

Figure 1(b) plots the energy flows for $(J, \Delta) = (0.1, 10.0)$ and the results show the behavior of the NFL fixed point for $N > 38$. In this case, each multiplet does not change $\{C\}$ with N , and the ground state is now doublet with $\{C\} = (0, 0)$. The first excited multiplet has 4 states with $\{C\} = (\pm 1, 0)$ or $(0, \pm 1)$, while the second excited multiplet has 10 states with $\{C\} = (0, 0), (\pm 1, 0)$, or $(0, \pm 1)$. This agrees with the spectrum at the NFL fixed point.⁵⁾ Thus, when the Γ_1 excitation energy becomes large $\Delta \gg J$, Γ_1 is effectively decoupled and the system is reduced to the ordinary quadrupole Kondo model with two symmetric spin channels.¹⁵⁾

The J - Δ phase diagram is determined following the above procedure and the result is shown in Fig. 2. The LFL and NFL phases are separated by a smooth boundary $J_c(\Delta)$ that becomes straight at large Δ . This can be understood by considering the strong coupling limit, which is described by the local term H_0 . We can easily diagonalize it and find a singlet ground state for $J/\Delta > \frac{2}{27} = R_c$ and doublet ground state for $J/\Delta < R_c$. The degeneracy is elevated to triplet at the level crossing point. It is clear that the asymptotic form in the large- Δ region is $J_c \sim R_c \Delta$. The small coupling part (small Δ and J) is most interesting, but it is not easy to precisely determine $J_c(\Delta)$ due to slow convergence in the NRG iterations that is enhanced by a small energy scale. The boundary shows a singular Δ -dependence near the origin. If this dependence is a simple power $J_c \sim \Delta^\alpha$, the exponent may be determined by analyzing the three data points for the smallest Δ values, and the result is $0.15 < \alpha < 1.4$ despite rough estimate due to large error bars. For fitting the boundary in the whole range of $0 < \Delta < 10$, we have tried several functions and the result is quite nice with $J_c = (a_2\Delta^2 + a_3\Delta^3 + a_4\Delta^4)^{1/4}$, where $a_2 = 0.0013(1)$, $a_3 = 0.58(9) \times 10^{-4}$, and $a_4 = 0.27(12) \times 10^{-4}$. Its small- Δ asymptotic form is a power with the exponent $\alpha = 1/2$, which falls in the window determined above. Finally, the $J = 0$ part of the phase diagram is the free electron phase where the local impurity is completely decoupled from conduction electrons.

The EQKM has two phases in the parameter space even

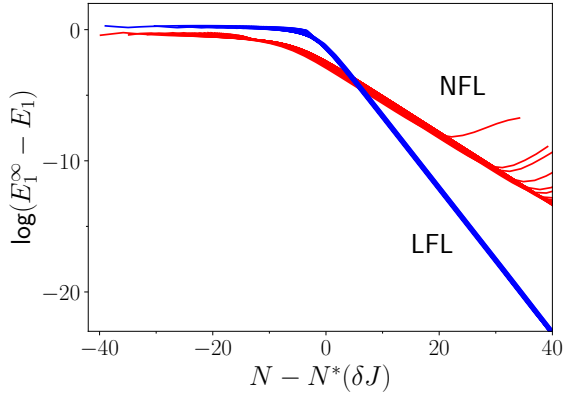


Fig. 3. (Color online) NRG energy flows for 101 J -points at $\Delta = 1.0$ in the LFL region (blue) and for 40 J -points at $\Delta = 2.0$ in the NFL region (red). $\delta J \equiv J - J_c(\Delta)$. The step number is shifted by $N^*(\delta J)$.

though the system does not change its channel symmetry, and this differs from the canonical behavior of the two-channel spin Kondo model. In order to explore other novel behaviors, we investigate in detail the scaling of the Kondo temperature $T_K(J)$ in the LFL phase near the phase boundary. To define T_K , we follow Wilson's original idea of crossover and keep track of the NRG flow of some energy level.^{3,5} The ground state belongs to the subspace of $\{C\} = (0, 0)$. We here choose the energy of the first excited state in this subspace and record its energy flow $E_1(N)$ with the NRG step N . Note that the scaling of $T_K(J)$ does not depend on the choice of this eigenstate, since all the low-energy states show a common convergence behavior in the $N \rightarrow \infty$ limit. The chosen one is the state that shows the simplest convergence behavior even for not large N and thus the easiest to analyze. We then define the crossover step N^* by the relation $E_1(N^*) = (1 \pm \frac{1}{5})E_1^\infty$, where E_1^∞ is the value at the strong coupling fixed point. In practice, we fitted $E_1(N)$ by the function $E_1^\infty + b_1\Lambda^{-N/2} + b_2\Lambda^{-N}$ and obtained a fractional value for N^* and defined the Kondo temperature by $T_K = t\Lambda^{-N^*/2}$. The energy unit is set to $t = 1$ as explained before. Figure 3 shows the energy flow of $E_1(N)$ for 101-points in the region $0.010 < J - J_c(\Delta) < 0.111$. All the plots fall on the universal curve within small numerical errors, and this confirms that the low-energy physics is governed by the same fixed point.

The scaling form of the Kondo temperature is $T_K \sim A'J^{b'} \exp(-c'/J)$ with $b' = 1/2$ for the simplest case, *i.e.*, the spin-1/2 single-channel Kondo model (SCKM).³ Let us first examine whether T_K in the EQKM follows this scaling. Note that J should be replaced by the distance from the phase boundary δJ . Figure 4 (a) shows the scaled form $f(\delta J) = \delta J \log[T_K(J)/\delta J^{b'}]$ for the fixed value $\Delta = 1$. If the above scaling works, $f(\delta J)$ should show a straight line, but the result for $b' = 1/2$ is very nonlinear and this indicates a different scaling form. To check this point, we repeated the same procedure for the SCKM to determine its T_K and plotted the result in the same panel. This time, the result shows a nice linear behavior confirming the expected scaling form for the SCKM.

We have tried many scaling functions for fitting $T_K(J)$ of the EQKM. It turned out that the most promising one was a stretched exponential $F(\delta J) \exp(-c/\sqrt{\delta J})$ with the prefactor

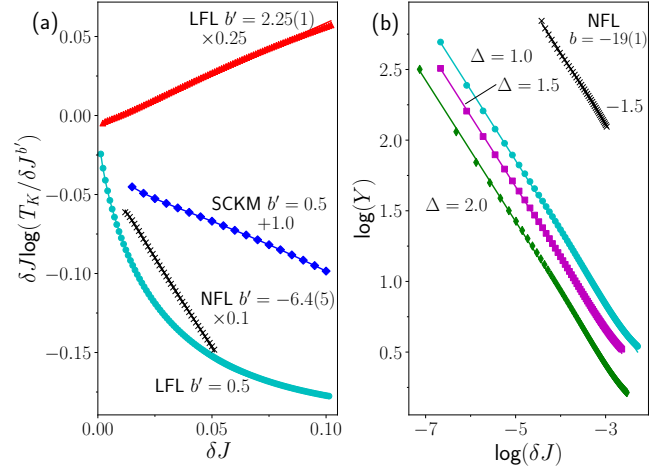


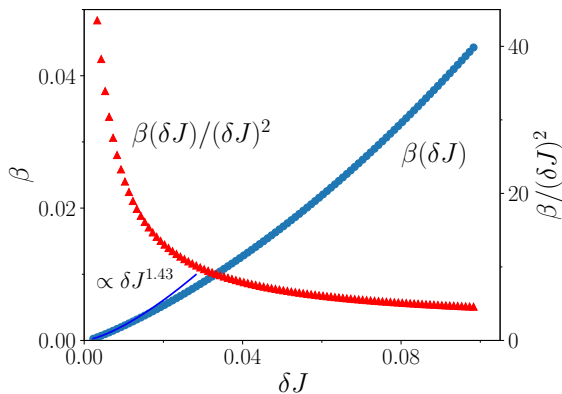
Fig. 4. (Color online) Scaling of the Kondo temperature T_K . (a) $\delta J \log(T_K/\delta J^{b'})$ vs $\delta J = J - J_c(\Delta)$. The results of the EQKM in the LFL and NFL phases are compared with those of the SCKM. Some data are shifted vertically, while some other are multiplied by a factor. They are marked by “+1.0” or “ $\times 0.25$ ” etc. (b) Double-logarithmic plot of $Y(\delta J)$ for the EQKM. $Y = -\log[T_K/(A(J - J_c(\Delta))^{b'})]$ using the parameters in Table I. The slope of the lines coincides with the expected exponent $1/2$ in the stretched exponential. The curve of the NFL phase is shifted downwards by 1.5.

$F(\delta J) = A(\delta J)^{b'}$. The parameters are optimized by minimizing fitting error for $\log T_K$, and the results are listed in Table I for three Δ values. Using these optimized parameters, Fig. 4(b) shows $Y = -\log[T_K/F(\delta J)]$, which is expected close to $\sqrt{\delta J}/c$. If this is the case, the double-logarithmic plot of $Y(\delta J)$ should show a straight line with slope $\frac{1}{2}$, and one can see that this works nicely in the panel (b). Another promising scaling function is an ordinary Kondo form with a generalized exponent shown in Fig. 4(a). The fitting error is minimized to 0.463 by using the exponent $b' = 2.25(1)$ together with $\log A' = 2.59(4)$, $c' = 0.0244(2)$, and $J_c = 0.210(1)$, but this form is unacceptable. Recall $1/c'$ corresponds to the effective conduction electron density of states, and its value seems unphysically large. Another reason is that the fitting error is more than 3 times larger than the case of stretched exponential form. These facts strongly support the proposed stretched exponential for the best scaling function.

In order to consider the origin of the stretched exponential scaling, it is instructive to recall that this type of scaling also appears at the Kosterlitz-Thoules transition,²⁸ which is governed by two parameters (*i.e.*, stiffness $\delta K = K - K_c$ and vortex fugacity g). Their RG equations have the β -functions which start from the second-order terms, and this is common to those of the SCKM with spin anisotropy.²⁹ As the bare couplings change with temperature T and cross the separatrix line at T_{KT} , the scaling function shows the factor $\exp(\pm \text{const.}/\sqrt{T - T_{KT}})$ in the disordered phase. Thus, we may expect that the RG equations of multiple coupling constants explain the observed scaling behavior if their β -functions have a proper form. It is natural to consider three effective coupling constants for the present EQKM. One is the excitation energy Δ and the other two are quadrupole exchange constants J_{33} and J_{31} . The impurity quadrupole operators in H_0 consist of two parts: $Q_\mu = Q_\mu^{(33)} + aQ_\mu^{(31)}$ ($\mu = z, x$) where $a = \sqrt{35}/2$ is the amplitude of $\Gamma_3 - \Gamma_1$ transition. At each

Table I. Optimized parameters including $J_c(\Delta)$ for fitting T_K in the EQKM with a stretched exponential form.

Δ	$\log A$	b	c	J_c
1.0	2.23(3)	1.49(1)	0.525(3)	0.211(1)
1.5	2.07(3)	1.51(1)	0.436(3)	0.249(1)
2.0	1.96(3)	1.51(2)	0.341(2)	0.284(1)

**Fig. 5.** (Color online) β -function of the EQKM for $\Delta = 1.0$. The used $J_c(\Delta)$ value is taken from Table I.

RG operation, their exchange couplings J_{33} and J_{31} are renormalized and the renormalization is generically different between them. Construction and analysis of their RG equations is an important step for a better understanding of the unconventional scaling in the EQKM. However, it is beyond the scope of the present study and we leave it for future study.

Following the same procedure, we also analyzed the Kondo temperature in the NFL phase at $\Delta = 2.0$. We once again used the energy of the first excited state $E_1(N)$ in the subspace $\{C\} = (0, 0)$ to determine T_K using the same definition.³⁰ The energy flow is shown in Fig. 3 for 40 points in the region $0.012 < \delta J < 0.051$. All the plots once again fall on the universal curve. This time, however, some plots move away for large $N - N^*(\delta J)$, but this is due to numerical errors. In the NFL phase, the ground state is a doublet and they appear in the same $\{C\}$ subspace. Numerical errors lift this degeneracy and destabilize the RG flows. Figure 3 shows the asymptotic slope $-0.2473(2)$ different from the value $-1/2$ in the LFL region. This indicates the RG eigenvalue $y \sim -1/4$ for the leading irrelevant operator around the NFL fixed point. Figures 4(a) and (b) show that the proposed scalings work quite reasonably. However, the determined value of the exponents $b' = -6.4(5)$ and $b = -19(1)$, seem unphysical. This may indicate the possibility of another new scaling behavior distinct, but we also leave this point for future studies.

We can further confirm the different T_K scaling in the LFL phase of the EQKM by analyzing an effective β -function. Suppose T_K is determined by the RG equation of one parameter $\delta J(N)$ alone, $d\delta J/dN = \beta(\delta J)$, as in the case of the SCKM. Then, the definition $T_K = \Lambda^{-N^*/2}$ leads to the relation $\beta = (\log \Lambda/2)[d(\log T_K)/dJ]^{-1}$ evaluated at $J = J_c + \delta J$. We numerically calculated this and the determined $\beta(\delta J)$ is shown in Fig. 5. As for the SCKM, it is known that the β -function starts

from a marginally relevant term $\beta(J) = \rho J^2 + c_3 J^3 + \dots$.³¹⁾

The determined $\beta(\delta J)$ apparently differs from this conventional form, as shown by a divergent behavior of $\beta/(\delta J)^2$. The small- δJ part is approximated by a simple power $(\delta J)^\nu$ with the fractional exponent $\nu = 1.43(3)$. This nonanalyticity of the effective β -function exhibits a failure of a single RG equation. Thus, one needs to consider coupled RG equations of multiple coupling constants, which was also anticipated from the determined scaling function of stretched exponential form.

In summary, we have performed the NRG study on the quadrupole Kondo effect with taking into account the crystal-field Γ_1 singlet state with excitation energy Δ . The determined phase diagram has two phases, local Fermi liquid for $J \gg \Delta$ and non-Fermi liquid for $J \ll \Delta$. We have also found a new scaling form of the Kondo temperature in the local Fermi liquid phase, and it is a stretched exponential function. To achieve a full understanding of this behavior, we need to analyze the RG equations of multiple coupling constants and explore a related boundary conformal theory as well as perform numerical calculations with higher precision. They are important future studies.

Acknowledgements The main part of numerical calculations was performed using the facility at the Supercomputer Center, ISSP, the University of Tokyo.

- 1) P. Nozières and A. Blandin, J. Phys. (Paris) **41**, 193 (1980).
- 2) P. Nozières, J. Low Temp. Phys. **17**, 31 (1974).
- 3) K. G. Wilson, Rev. Mod. Phys. **47**, 773 (1975).
- 4) R. Bulla, T. A. Costi, and T. Pruschke, Rev. Mod. Phys. **80**, 395 (2008).
- 5) H. B. Pang and D. L. Cox, Phys. Rev. B **44**, 9454 (1991).
- 6) I. Affleck, Nucl. Phys. B **336**, 517 (1990).
- 7) I. Affleck and A. W. Ludwig, Nucl. Phys. B **352**, 849 (1991).
- 8) I. Affleck and A. W. Ludwig, Phys. Rev. Lett. **67**, 161 (1991).
- 9) I. Affleck and A. W. Ludwig, Nucl. Phys. B **360**, 641 (1991).
- 10) N. Andrei and C. Destri, Phys. Rev. Lett. **52**, 364 (1984).
- 11) A. M. Tsvelick and P. B. Wiegmann, J. Stat. Phys. **38**, 125 (1985).
- 12) P. Schlottmann and P. D. Sacramento, Physica B **206**, 95 (1995).
- 13) D. M. Cragg, P. Lloyd, and P. Nozières, J. Phys. B **13**, 803 (1980).
- 14) I. Affleck, A. W. Ludwig, H. B. Pang, and D. L. Cox, Phys. Rev. B **45**, 7918 (1992).
- 15) D. L. Cox, Phys. Rev. Lett. **59**, 1240 (1987).
- 16) D. L. Cox, Physica C **153**, 1642 (1988).
- 17) D. L. Cox, J. Magn. Magn. Mater. **76**, 53 (1988).
- 18) A. Sakai and S. Nakatsuji, J. Phys. Soc. Jpn. **80**, 063701 (2011).
- 19) T. Onimaru, K. T. Matsumoto, Y. F. Inoue, K. Umeo, T. Sakakibara, Y. Karaki, M. Kubota, and T. Takabatake, Phys. Rev. Lett. **106**, 177001 (2011).
- 20) T. Onimaru, K. Izawa, K. T. Matsumoto, T. Yoshida, Y. Machida, T. Ikeura, K. Wakiya, K. Umeo, S. Kittaka, K. Araki, T. Sakakibara, and T. Takabatake, Phys. Rev. B **94**, 075134 (2016).
- 21) A. Tsuruta and K. Miyake, J. Phys. Soc. Jpn. **84**, 114714 (2015).
- 22) Y. Yamane, T. Onimaru, K. Wakiya, K. T. Matsumoto, K. Umeo, and T. Takabatake, Phys. Rev. Lett. **121**, 077206 (2018).
- 23) K. Hattori and H. Tsunetsugu, J. Phys. Soc. Jpn. **83**, 034709 (2014).
- 24) M. Koga and H. Shiba, J. Phys. Soc. Jpn. **64**, 4345 (1995).
- 25) M. Koga and H. Shiba, J. Phys. Soc. Jpn. **65**, 3007 (1996).
- 26) M. Koga and H. Shiba, J. Phys. Soc. Jpn. **66**, 1485 (1997).
- 27) H. Kusunose, J. Phys. Soc. Jpn. **67**, 61 (1998).
- 28) J. M. Kosterlitz and D. J. Thouless, J. Phys. C **6**, 1181 (1973).
- 29) A. C. Hewson, *The Kondo Problem to Heavy Fermions* (Cambridge University Press, 1993).
- 30) D. L. Cox and A. Zawadowski, Adv. Phys. **47**, 599 (1998).
- 31) P. W. Anderson, J. Phys. C **3**, 2436 (1970).